

See discussions, stats, and author profiles for this publication at: <https://www.researchgate.net/publication/283462964>

Survey on electrical modeling methods applied on different battery types

Conference Paper · April 2015

DOI: 10.1109/TAECE.2015.7113597

CITATIONS

28

READS

2,337

5 authors, including:



Nagham El Ghossein

École Catholique d'Arts et Métiers

13 PUBLICATIONS 132 CITATIONS

[SEE PROFILE](#)



Jack P. Salameh

La Rochelle Université

10 PUBLICATIONS 215 CITATIONS

[SEE PROFILE](#)



Nabil Karami

Lebanese University

28 PUBLICATIONS 698 CITATIONS

[SEE PROFILE](#)



Moustapha H El Hassan

University of Balamand

38 PUBLICATIONS 301 CITATIONS

[SEE PROFILE](#)

Some of the authors of this publication are also working on these related projects:



Real generation of power quality disturbances [View project](#)



Aging modeling and lifetime prediction of Lithium-Ion Capacitors (LIC). [View project](#)

Survey on Electrical Modeling Methods Applied on Different Battery Types

Nagham El Ghossein, Jack P. Salameh, Nabil Karami, *Member, IEEE*, Moustapha El Hassan, *Member, IEEE*,
Maged B. Najjar, *Member, IEEE*

Department of Electrical Engineering
University of Balamand
Koura, Lebanon

naghamghossein@gmail.com, jacksalameh@live.com, nabilkarami@hotmail.com, moustapha.elhassan@balamand.edu.lb

Abstract—The evolution of battery management systems has imposed the necessity of evaluating batteries equivalent circuit models. The advantage of this type of modeling is to accurately estimate the dynamic aspects of a battery. Circuit parameters are identified for the purpose of forecasting different battery states. This paper presents multiple circuit models described in the literature. Four types of batteries are studied: Nickel-Metal Hybrid, Lithium-Ion, Lead-acid and Lithium Polymer.

Keywords—Batteries; circuit model; Nickel-Metal; Lithium Ion; Lead-acid; Lithium Polymer.

I. INTRODUCTION

Battery usage is becoming very abundant in the modern days. Due to the complexity of the electric power systems put on the market nowadays (EV, HEV...), and with the need to find optimal operation strategies, it has become of a major importance to be able to monitor battery behavior and parameters. All mobile systems depend on the energy stored within the device to function, as electric vehicles, smartphones, laptops etc. Furthermore, the urgent need to find renewable sources of energy turned the attention towards batteries as the only device capable of storing energy.

Battery modeling was the key in recent years in the improvement of charging/discharging techniques and enhancement of battery capacity and density. However, predicting the battery lifespan remains a problematic due to the lack of a routine able to execute such a prediction. Nevertheless, the numerous models developed during the past two decades were useful in reaching an integrated battery testing and simulation capability. Various battery models were developed for the purpose of studying, estimating or predicting the real-time operation of the battery. These battery models are of four categories [1]:

- Electrochemical models: known to be the most accurate yet tedious to configure, they use coupled nonlinear differential equations to describe the chemical reactions taking place in the battery.
- Analytical models: they use simplified reduced number of equations than the electrochemical model. The analytical models monitor the nonlinear relationship between the real-time operation of the battery and the

rate of discharge without taking the recovery effect into account.

- Stochastic models: they focus on modeling the recovery effect and behavior of the battery as a Markov process with probabilities function of the parameters related to the physical characteristics of an electrochemical cell.
- Electrical Models: they represent the battery in an equivalent electrical circuit while the composing elements are voltage and current sources, resistors and capacitors. Electrical circuit models are good for simulation. However, they neglect the nonlinear capacity behavior resulting an inaccuracy in predicting the remaining battery capacity and operating time [2].

This paper presents numerous simple and advanced electrical models of the four most used batteries in the industry: Nickel-Metal Hybrid, Lithium-ion, Lead Acid and Lithium Polymer. In section II several models of the four batteries are introduced while finding a common model that can be used to simulate the behavior of all batteries. A discussion and a conclusion are presented in Section III and IV, respectively.

II. ELECTRICAL MODEL

Numerous electrical models are developed for batteries in order to identify the lifespan of the battery. An emerging theory is tackling the internal parameters of the battery as the resistance and capacitance, as a way of observing the rate of change of the parameters and their effect on the efficiency of the battery in order to find a relation between the parameters' values and the battery lifespan. This can be done either by simulation of the electrical model, or experimental measures on different batteries for different interval of time.

A. Nickel-Metal Hybrid (NiMH)

This is a rechargeable battery with its chemical reactions similar to the Nickel-Cadium (NiCd), however it has two to three times the capacity of NiCd. The electrical model for the

NiMH is similar to the NiCd's derived by Notten [3-5] and based on [6], the NiMH model is shown in Fig.1.

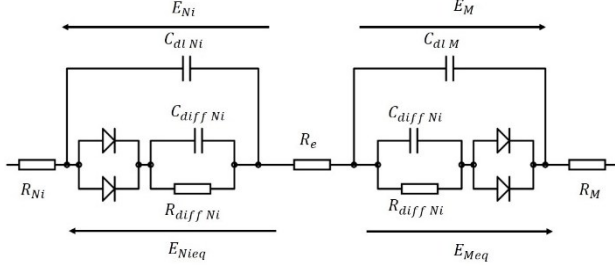


Fig. 1. Battery model of NiMH based on the Notten model for NiCd.

where, E_{Nieq} and E_{Meq} represent the equilibrium voltages of the Nickel and Metal electrodes respectively, R_{Ni} and R_M represent the connective resistances of the Nickel and Metal electrodes respectively, R_e is the electrolyte resistance and C_{dlNi} and C_{dlM} represent the double layer capacitors.

The diodes correspond to the phenomenon of charge transfer. The combination of $(C_{diffNi} // R_{diffNi})$ and $(C_{diffM} // R_{diffM})$ are related to the diffusion phenomenon.

In order to reach the electrical model, the electrochemical reactions are globally considered. Thus based on the equivalent circuit found by Randles [7], and considering E_0 to be the total equilibrium voltage of the NiMH cell, the equivalent circuit is shown in Fig.2.

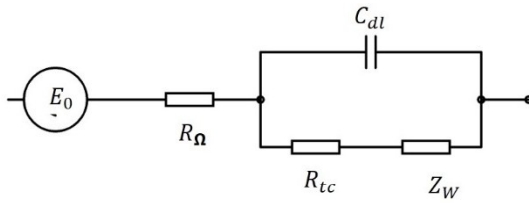


Fig. 2. Randles equivalent circuit for the NiMH battery.

In the Randles equivalent circuit the time constant τ , equal to $R_{tc}C_{dl}$ relative to the charge transfer phenomenon, is smaller than the time constant of the diffusion phenomenon. Therefore, the modified Randles circuit model is shown in Fig.3, where, Z_w is the Warburg impedance.

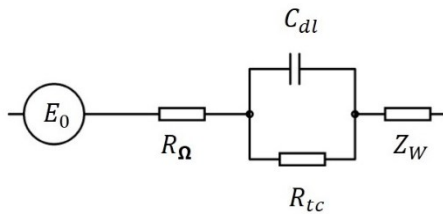


Fig. 3. Randles equivalent circuit for the NiMH battery.

Moving into frequency domain the total equivalent impedance Z_T is found to be:

$$Z_T(s) = R_{\Omega} + \frac{R_{tc}}{1 + s R_{tc} C_{dl}} + Z_W(s)$$

In order to find the expression of the Warburg impedance, spectroscopy measurements are performed on the single NiMH element at several State Of Charge (SOC) [8]. The spectroscopy measurements are executed by applying a low sinus voltage with an amplitude near 10 mV to the equilibrium voltage of the cell at a given SOC. The current will flow in the cell at the same frequency but with a phase shift. Dividing the expressions of voltage and current will lead to the total impedance of the cell.

$$Z_T(s) = \frac{V_{max}}{I_{max}} e^{j\phi}$$

The impedance spectrum of the cell is found while changing the frequency at a definite SOC. In low frequencies, the gain of $Z_T(s)$ can be reached by two asymptotes drawn on the bode plot, one of which is a non-integer integrator H_1 , the other is a high pass function H_2 , where:

$$H_1(s) = \frac{1}{(\tau_1 s)^{n_1}}$$

$$H_2(s) = (1 + \tau_2 s)^{n_2}$$

The expression of the Warburg impedance is deduced from the product of these two functions.

$$Z_w(s) = H_1(s)H_2(s) = \frac{(1 + \tau_2 s)^{n_2}}{(\tau_1 s)^{n_1}}$$

After determining $Z_w(s)$ one can find the voltage $V(t)$ as a response to an echelon current $I(t)$.

$$V(t) = E_0 + R_{\Omega}I(t) + R_{tc} \left(1 - e^{-\frac{t}{R_{tc}C_{dl}}} \right) I(t) + L^{-1} \left(\frac{(1 + \tau_2 s)^{n_2}}{(\tau_1 s)^{n_1}} I(s) \right)$$

The model in Fig.2 considers only one cell of the battery NiMH. The overall expression of pack with n cells can be derived by multiplying the expression of $V(t)$ by n while finding the equivalent voltage of the pack as shown in Fig.4.

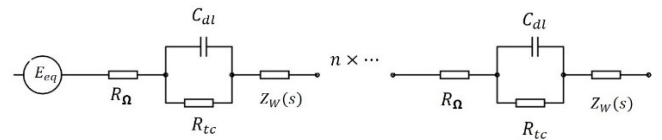


Fig. 4. Randles equivalent circuit for the NiMH battery with n cells.

This type of batteries can also be modelled by Thevenin model described in the following sections.

B. Lithium-ion (Li-ion)

One can represent the equivalent circuit model for Li-ion battery as a combination of voltage source, resistors and capacitors. The battery dynamics is described by RC ladders. The accuracy of the model will increase while adding more RC cells but with more complexity [9]. To begin with the simplest model called Thevenin model is considered in Fig.5.

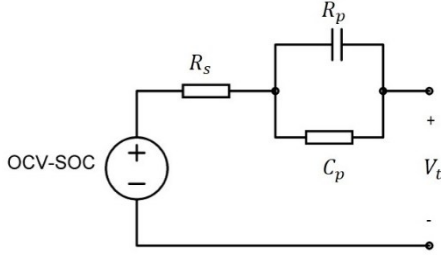


Fig. 5. Simplest model for Li-ion batteries.

The state space model of the circuit can be derived with the voltage across the ladder being U_p .

$$\begin{bmatrix} \dot{SOC} \\ \dot{U}_p \end{bmatrix} = \begin{bmatrix} 0 & 0 \\ 0 & -\frac{1}{R_p C_p} \end{bmatrix} \begin{bmatrix} SOC \\ U_p \end{bmatrix} + \begin{bmatrix} -\frac{1}{C_n} \\ \frac{1}{C_p} \end{bmatrix} I$$

where,

$$SOC(t) = SOC(t_0) - \int_{t_0}^t \frac{I(\tau)}{C_n} d\tau$$

With C_n being the battery capacity, $I(t)$ is the battery current with a positive value while discharging. In addition the total output voltage V_t in figure 5 is found to be:

$$V_t = OCV(SOC) - U_p - R_s I$$

The resistance R_s is calculated by the ratio of the instantaneous voltage drop and the discharging current at the instant when the discharging current starts. R_s has the similar value in the whole SOC range.

$$R_s = \frac{V(R_s)}{I}$$

Based on the solution of the differential equation of U_p , the voltage curve of each transient period is approximated by:

$$V_t = OCV + ae^{bt}$$

where, a and b are determined based on the curve fitting. One, therefore, can find the values of R_p and C_p as follows:

$$R_p = -\frac{a}{I} \text{ and } C_p = -\frac{1}{R_p b}$$

Based on Electrochemical Impedance Spectroscopy (EIS), the equivalent complex circuit can be divided into three parts consisting of a series resistance, a charge transfer and double layer reaction, and a diffusion process in terms of the frequency components [10].

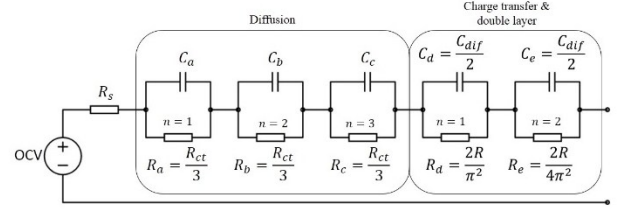


Fig. 6. Lumped equivalent circuit model of Lithium-Ion battery.

The impedance spectra of the charge transfer and diffusion parts are constantly varying based on the operating conditions of the battery. All battery parameters are functions of the operating conditions, such as current, the SOC and the temperature.

Introducing the Warburg impedance into the model of the Lithium-Ion battery, the circuit would become more complex but of course much more accurate [11]. The circuit of the Lithium-Ion battery while taking into account the Warburg impedance is in Fig.7.

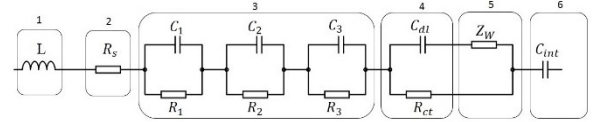


Fig. 7. Equivalent circuit of Lithium-ion battery with Warburg impedance.

- (1) Line induction and induction from spiral wound nature of cell.
- (2) The ohmic resistance of solution and contacts.
- (3) Solid-electrolyte interface (SEI) layer growth
- (4) Charge transfer kinetics.
- (5) Ionic diffusion.
- (6) Mass capacitance of electrode.

The Warburg resistance and capacitance are expressed as:

$$R_w = \sum_{1}^n r_w \text{ and } C_w = \sum_{1}^n c_w$$

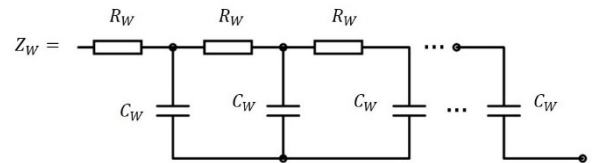


Fig. 8. Warburg impedance.

The mathematical Warburg representation is as follows:

$$Z_w(\omega) = R_w \frac{\tanh(j\omega T_w)^p}{(j\omega T_w)^p}$$

where,

$$T_w = R_w C_w$$

The battery's performance in the time domain is found by transforming the electric circuit model in frequency domain using Fourier transform technique to reach the following model.

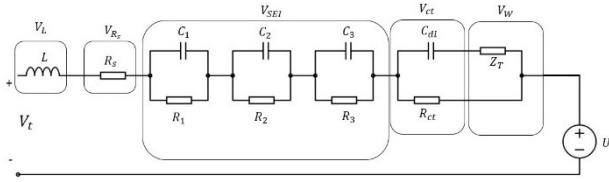


Fig. 9. Time domain equivalent circuit of the Lithium-Ion battery.

The Warburg impedance is approximated into Z_T by the RC ladder network. The values of R_{Tn} and C_{Tn} in Fig.10 are found from a simple conversion of the Warburg element into a time domain transmission model as:

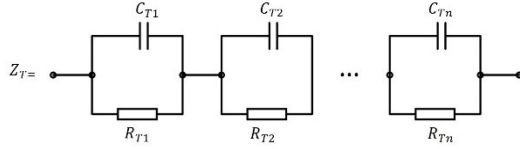


Fig. 10. Total impedance Z_T .

$$R_{Tn} = \frac{8R_w}{(2n-1)^2\pi^2} \quad \text{and} \quad C_{Tn} = \frac{C_w}{2}$$

C. Lead-acid

Lead-Acid Batteries are extensively employed in the structure of electric vehicles. They store or deliver energy in several electrical systems. The chemical energy stored inside the battery is translated into electrical energy. When the battery is over-discharged, the battery is damaged because "sulfation" takes place. In case lead-sulfate is formed in large quantities, the chemical reaction inside the battery is not reversible anymore [12].

A lead-Acid battery can be modeled by different circuit models. The dynamic behavior of a lead-acid battery can be represented by the most common model of a battery, Thevenin's equivalent circuit model in Fig.11 [13-14].

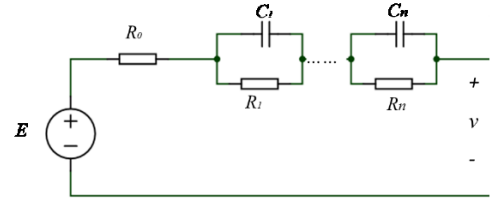


Fig. 11. Thevenin equivalent circuit model.

The components of Fig.11 depend on many factors: the SOC, the load current, the temperature and the charge/discharge behavior. Under some precise conditions, the parameters do not vary for a short duration. The internal resistance R_0 is the resistance of contacts, electrodes and electrolyte. The RC parallel blocks represent the charge transfer and the double layer reaction. E is the open circuit voltage. When the model consists of n parallel RC blocks, it is called a Thevenin model of order n .

Thevenin model does not manifest the open circuit voltage diminution during discharge. Therefore, E is replaced by a capacitance C_0 as illustrated in Fig.12 [15].

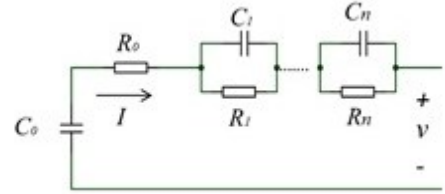


Fig. 12. Equivalent circuit model during charge.

This model can outline the charging behavior of a lead-acid battery. The terminal voltage of the model connected to a constant load is:

$$v(t) = v(0^-) - \frac{I}{C_0}t - R_0I - \sum_{k=1}^n R_kI(1 - e^{-\frac{t}{R_kC_k}})$$

Moreover, for the self-discharging dynamics representation, the constant voltage source of the Thevenin model is replaced by a parallel RC block as shown Fig.13.

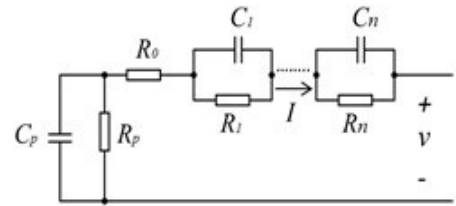


Fig. 13. Equivalent circuit model during discharge

The terminal voltage is then described by the following equation:

$$v(t) = e^{-\frac{t}{R_p C_p}} v(0^-) - R_0 I - R_p I \left(1 - e^{-\frac{t}{R_p C_p}} \right) - \sum_{k=1}^n R_k I (1 - e^{-\frac{t}{R_k C_k}})$$

where, R_k and C_k are the k^{th} resistor and capacitor.

The efficiency of a specific model depends primarily on the working conditions. A simple model of a lead-acid battery is described in [16]. It consists of a controlled voltage source E in series with a resistance. E is dependent on points extracted from the discharge characteristics curve given by the manufacturer. Note that for a lead-acid battery, the hysteresis phenomenon is illustrated in the discharge curve. E is defined by the two following equations for charge and discharge respectively.

$$E(t) = E_0 - Ri(t) - K \frac{Q}{it - 0.1Q} i^* - K \frac{Q}{Q - it} it + e^t$$

$$E(t) = E_0 - Ri(t) - K \frac{Q}{Q - it} (it + i^*) + e^t$$

where, E_0 is the battery constant voltage, K is the polarization constant, Q is the battery capacity, it is the actual battery charge (integral of the current with respect to time), e^t is the exponential zone voltage, $i(t)$ is the battery current and i^* is the filtered current.

D. Lithium Polymer (LiPo)

A Lithium Polymer battery consists of several components [17]:

- Positive Electrode consisting of LiCoO_2 or LiMn_2O_4 .
- Separator made of a liquid electrolyte that contains LiPF_6 and organic solvents.
- Negative Electrode formed by carbon material.

This type of battery has a thin design while still having relatively good battery life, a very lightweight and an advanced safety. However, these batteries are more costly for manufacturing than lithium-ion batteries.

A LiPo battery can be represented by a simplified battery model similar to Fig. 5; an internal resistance in series with one parallel $R_p C_p$ block [18]. V_{oc} is the open circuit voltage, R_s is the internal resistance, R_p and C_p represent the multiple RC parallel blocks. This open circuit voltage can be expressed by the following equation when the battery is connected to a resistive load.

$$V_{oc} = V_t + (R_s + R_p)I - R_p I e^{\frac{t}{R_p C_p}}$$

This model merges a mathematical part, V_{oc} , in the electrical circuit model because the open circuit voltage is related to the state of charge of the battery.

Equivalent circuit model of Fig.5 is also adopted in [19]. However, parameters are manipulated in a different way. The open circuit voltage is described by the following equation:

$$V_{oc} = E_0 - K \frac{Q}{Q - \int idt} + A e^{(-B \int idt)}$$

where, E_0 is the battery constant voltage, K is the polarization voltage, Q is the battery capacity, A is the exponential zone amplitude and B is the exponential zone time constant inverse. A and B can be found from the battery characteristic curve. This model combines Shepherd model, which characterizes the non linear open circuit voltage of a lithium polymer battery, and Thevenin Model.

In order to model a LiPo battery, two processes should be illustrated: static behavior, which is the ohmic state, and the dynamic behavior, which is the charge transfer and the double layer processes. Therefore, multiple components should be designed in order to emphasize the battery action more precisely such as: resistance, capacitance or *CPE* (constant-phase-element). The *CPE* represents the behavior of a double layer which is an imperfect capacitor. Therefore, an equivalent battery model is shown in Fig.15 as described in [20].

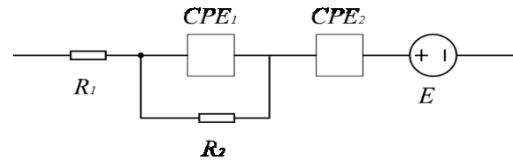


Fig. 14. Proposed battery model in [20].

where, E represents a voltage source which is dependent on SOC, R_1 is a resistance that illustrates the ohmic behavior, R_2 is a resistance having a nonlinear dependence on SOC, CPE_1 characterizes the overvoltage varying with time that occurs during charging or discharging, and CPE_2 describes the model diffusion behavior at low frequencies.

In this model, all components are variable according to the temperature. Parameters values are variable with temperature, state of charge, time and degradation. In fact, they are dependent on the operating point of the battery.

Another equivalent circuit model of lithium polymer battery is analyzed in [21]. The inductive component is added so the impedance increases in high frequencies and the admittance decreases, similarly to Fig.15. Therefore, this model is useful when having high frequency systems.

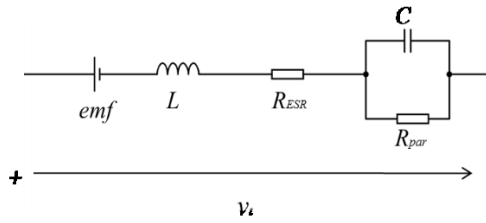


Fig. 15. LiPo circuit model for high frequency applications.

Let the input be the voltage applied to the battery and the output be the current passing through the battery. The transfer function of the model is:

$$G(s) = \frac{CR_{par}s + 1}{LCR_{par}s^2 + (L + CR_{ESR}R_{par})s + R_{ESR} + R_{par}}$$

III. DISCUSSION

Examining the different mentioned electrical models for the different types of batteries, one can comprehend that accuracy comes on the expense of simplicity in the model chosen. However, considering the complexity of the spectroscopy measurements, the model on which it is based takes into account the electrochemical reactions of the battery, but these reactions are prone to many external and internal factors; hence any simulation would never give the intended accurate result. In order to reach a compromise between accuracy and the ability to simulate, the Thevenin equivalent circuit comes in handy because of its simplicity and the ability of increasing its accuracy by adding more RC ladders to the model. In order to find the number of RC ladders required for each type of batteries, parameters of the equivalent circuit model have to be found and the number is chosen according to the minimal RMSE between the model voltage and the battery voltage.

IV. CONCLUSION

Numerous circuit models of batteries are studied in the literature. Grouped into four categories: electrochemical, analytical, electrical, and stochastic, models are illustrated for four types of batteries. The Thevenin is the most simulation-realization best model that can describe the behavior of all these types using one simple circuit while extending its accuracy by adding more RC ladders to the simulated circuit.

To derive all the characteristics of a specific battery, parameters of these models are identified. Consequently, the state of charge, the lifetime and the capacity of a battery are estimated and one can find the parameters of each battery under study.

REFERENCES

- [1] M. R. Jonkerden & Haverkort B. R. (2009). Which battery model to use? *Software, IET*, 3(6), 445-457.
- [2] M. Chen, & Rincon-Mora, G. A. *Accurate electrical battery model capable of predicting runtime and IV performance*. IEEE transactions on Energy conversion, 21(2), 504-511. (2006).
- [3] P.H.L. Notten, W.S. Kruijt and H.J. Bergveld. *Electronic network modeling of rechargeable batteries: Part II the NiCd system*. 191st Electromechanical Society Meeting Montreal, May 1997.
- [4] P.H.L. Notten, *Electronic-network modeling of rechargeable NiCd cells and its application to the design of battery management systems*, Journal of power sources 77: 143-158, 2000.
- [5] A. J. Bard, L. R. Faulkner, *Electrochemical methods: fundamentals and applications* (Vol. 2). New York: Wiley. (1980)
- [6] E. Kuhn, C. Forgez, and G. Friedrich. *Modèle pour accumulateurs NiMH en vue d'une application pour véhicule hybride électrique*. EPF, Novembre 2002.
- [7] J.R. Macdonald, *Impedance Spectroscopy: Old Problems and New Developments*, Electrochimica Acta, Vol. 35, No. 10, pp. 1483-1492, 1990.
- [8] E. Kuhn, C. Forgez, and G. Friedrich, *Electric equivalent circuit of a NiMH cell: Methods and Results*, Laboratoire d'Electromecanique de Compiègne (LEC). (2000)
- [9] D. Jiani, W. Youyi, and W. Changyun, *Li-ion Battery SOC Estimation using Particle Filter Based on an Equivalent Circuit model*. 2013 10th IEEE ICCA. Hangzhou, China. (2013)
- [10] J. Lee, J. Lee, O. Nam, J. Kim, and B. H. Cho, *Modeling and Real Time Estimation of Lumped Equivalent Circuit Model of a Lithium Ion Battery*. School of Electrical Engineering and Computer Science, Seoul, Korea. (2006)
- [11] M. Greenleaf, H. Li, J. P. Zheng, *Modeling of Li_xFePO_4 cathode li-ion batteries using linear electrical circuit model*. IEEE Transactions on sustainable energy. Vol. 4, No. 4, October 2003.
- [12] Z. M. Salameh, M.A. Casacca, W.A. Lynch. "A mathematical model for lead-acid batteries." IEEE Trans. on Energy conversion, 7(1), pp.93-98, 1992.
- [13] L. Devarakonda, H. Wang, T. Hu. "Parameter identification of circuit models for lead-acid batteries under non-zero conditions". American control conference. 2014.
- [14] N. Karami, N. Moubayed, "Smart Battery Charger Using a Bridgeless Boost AC/DC Converter", IEEE Colloquium on Humanities, Science and Engineering Research (CHUSER), 2014.
- [15] T. Hu, J. Hoeguk, "Simple algorithms for determining parameters of circuit models for charging/discharging batteries." Journal of Power Sources 233 (2013): 14-22.
- [16] O. Tremblay, Dessaint, L.-A. "Experimental Validation of a Battery Dynamic Model for EV Applications." World Electric Vehicle Journal. Vol. 3 - ISSN 2032-6653 - 2009 AVERE, EVS24 Stavanger, Norway, May 13 - 16, 2009.
- [17] Z. M., Salameh, & Kim, B. G. (2009, July). *Advanced lithium polymer batteries*. In Power & Energy Society General Meeting.. PES'09. (pp. 1-5), IEEE, 2009
- [18] M. Ceylan, T. Sankurt, A. Balıkcı, "A Novel Lithium-Ion-Polymer Battery Model for Hybrid/Electric Vehicles", IEEE, 2014.
- [19] B., K. C., Choi, S. C., Kim, J. H., Won, C. Y., & Jung, Y. C. *LiFePO₄ dynamic battery modeling for battery simulator*. IEEE International Conference on Industrial Technology (ICIT) (pp. 354-358), IEEE, 2014.
- [20] A. EDDAHECH, O. BRIAT, H. AL JED, "Li-Po Batteries Modeling for Mail Delivery Electric Vehicles". Vehicle Power and Propulsion Conference, IEEE, 2011.
- [21] J. Jang. *Equivalent Circuit Evaluation Method of Lithium Polymer Battery Using Bode Plot and Numerical Analysis*, IEEE Trans. on Energy conversion, Vol. 26, No. 1, March 2011.